Available online at www.sciencedirect.com
ScienceDirect
Applied Geochemistry 23 (2008) 895–913
Applied Geochemistry
www.elsevier.com/locate/apgeochem

Metal mobilization from base-metal smelting slag dumps in Sierra Almagrera (Almería, Spain)

Andrés Navarro [a,*], Esteve Cardellach [b], José L. Mendoza [a], Mercé Corbella [b], Luis M. Domènech [a]

[a] *Dep. Mec. de Fluidos, Universitat Politècnica de Catalunya, ETSEIT, Colón 11, 08222 Terrassa, Spain*
[b] *Dep. Geologia, Universitat Autònoma de Barcelona, 08193 Bellaterra, Spain*

Received 11 July 2006; accepted 29 July 2007
Editorial handling by R.B. Wanty
Available online 15 January 2008

Abstract

Smelting slags associated with base-metal vein deposits of the Sierra Almagrera area (SE Spain) show high concentrations of Ag (<5–180 ppm), As (12–750 ppm), Cu (45–183 ppm), Fe (3.2–29.8%), Pb (511–2150 ppm), Sb (22–620 ppm) and Zn (639–8600 ppm). The slags are mainly composed of quartz, fayalite, barite, melilite, celsian, pyrrhotite, magnetite, galena and Zn–Pb–Fe alloys. No glassy phases were detected. The following weathering-related secondary phases were found: jarosite–natrojarosite, cotunnite, cerussite, goethite, ferrihydrite, chalcanthite, copiapite, goslarite, halotrichite and szomolnokite. The weathering of slag dumps near the Mediterranean shoreline has contaminated the soils and groundwater, which has caused concentrations in groundwater to increase to 0.64 mg/L Cu, 40 mg/L Fe, 0.6 mg/L Mn, 7.6 mg/L Zn, 5.1 mg/L Pb and 19 μg/L As. The results of laboratory leach tests showed major solubilization of Al (0.89–12.6 mg/L), Cu (>2.0 mg/L), Fe (0.22–9.8 mg/L), Mn (0.85–40.2 mg/L), Ni (0.092–2.7 mg/L), Pb (>2.0 mg/L) and Zn (>2.5 mg/L), and mobilization of Ag (0.2–31 μg/L), As (5.2–31 μg/L), Cd (1.3–36.8 μg/L) and Hg (0.2–7 μg/L). The leachates were modeled using the numerical code PHREEQC. The results suggested the dissolution of fayalite, ferrihydrite, jarosite, pyrrhotite, goethite, anglesite, goslarite, chalcanthite and cotunnite. The presence of secondary phases in the slag dumps and contaminated soils may indicate the mobilization of metals and metalloids, and help to explain the sources of groundwater contamination.

1. Introduction

Metallurgical wastes such as slags from base-metal ore processing are potential acid-generating systems capable of containing and mobilizing high concentrations of metals and other inorganic substances. Thus, in areas contaminated by smelting activities, high amounts of As, Cd, Cu, Co, Cr, Fe, Mo, Ni, Pb, Sb, Zn and other minor elements introduced by the weathering of wastes can often be detected in soil and/or groundwater.

Mining, and associated mineral processing and beneficiation may have a notable impact on the environment, which depends on many factors, especially

* Corresponding author. Tel.: +34 937398264; fax: +34 937398101.
E-mail address: navarro@mf.upc.es (A. Navarro).

0883-2927/$ - see front matter © 2008 Elsevier Ltd. All rights reserved.
doi:10.1016/j.apgeochem.2007.07.012

the type of mining and the size of the operation (Bell and Donnelly, 2006). Nevertheless, in modern mining activities, mine wastes may be deposited at storage facilities which satisfy environmental requirements related to construction, operation, inspection, surveillance and management. In addition, the reclamation of contaminated sites is based on the application of several technologies, such as stabilizing wastes, selective leaching, soil washing, reactive layers and permeable reactive barriers (Blowes et al., 2000; Navarro et al., 2006a; Bhandari et al., 2007). However, as reflected in the present study, ancient mining and smelting wastes were disposed without any environmental control measures to prevent the dispersion of metals.

Smelting wastes, mainly slags, have traditionally been considered relatively unreactive materials because the potential contaminants are encapsulated in low-solubility compounds such as silicates, oxides and glassy forms. However, recent studies have shown that smelter slags can be reactive and may be the source of metals and metalloids such as Ag, As, Ba, Cd, Cu, Pb, Sb and Zn in stream, soil and groundwater contamination (Parsons et al., 2001; Piatak et al., 2004). Slag deposits can be leached by surface waters or rising water tables in unconfined aquifers, thereby releasing contaminants to the soil, groundwater, sediments, reservoirs and drainage networks.

Mining has been a very important activity in SE Spain since the Roman age, especially in the Cartagena–Mazarrón and Sierra Almagrera areas (Navarro et al., 2004). Slags from Ag–Pb mining in these areas contain up to 5–7 wt.% Pb, 3–7 wt.% Zn and 0.02–0.04 wt.% As. Some of these elements have migrated into adjacent soils and river sediments, been taken up by plants, and been distributed by smelter plumes from furnaces to distant soils (Schmidt et al., 2001).

In other European countries, slag waste from historical Pb smelting facilities is also a source of metal and trace element contamination (Maskall et al., 1996). Heavy metal and metalloid pollution (Pb, Zn, Cd, Cu, As and Sb) has also been detected in the vicinity of lead smelters in Central Europe (Rieuwerts and Farago, 1996), with Pb concentrations of up to 37,300 ppm in soils.

Mineralogically, the furnace products of base-metal smelting show the following primary phases: spinels, Zn-rich fayalite, Zn-rich Ca–Fe silicates, melilite, corundum, apatite, metal oxides, metallic Fe, Pb, Cu and Zn; Fe–Zn alloys; carbides; phosphides; Fe, Zn, Pb, Cu and Mn sulfides; and Fe arsenides (Kucha et al., 1996). Frequent secondary phases include hydrated Fe sulfates, metal oxides and hydroxides and chlorides. Also, glass phases are very common, especially in granulated slags.

The source of metal contamination in soils and groundwater can be related to any metal-bearing phase (primary or secondary) present in the slags. Through geochemical modeling of field and laboratory data on slags from Penn Mine (California), Parsons et al. (2001) demonstrated that the main processes that control dissolved metal concentrations are the dissolution of metal-bearing silicates and glass, the precipitation of secondary phases, and sulfide oxidation. Thus, data from field and laboratory studies were used to develop kinetic geochemical models which suggest the importance of kinetic control for abiotic sulfide oxidation and surface-controlled dissolution of silicates, oxides and glass. Piatak et al. (2004) reached a similar conclusion on slags from massive sulfide deposits of the Vermont Cu belt and Idaho Pb–Ag deposits.

In semiarid regions like the present study area, leachate from slags can result in the formation of soluble sulfate minerals, which may precipitate directly from acid sulfate waters during dry periods. The formation of secondary phases (jarosite, gypsum, goethite, ferrihydrite, etc.) may control the distribution of trace elements in pore water by means of reactions such as adsorption, surface complexation and co-precipitation. During rainy periods, the trapped metals may be released from the hosting soluble phases and introduced into the environment, thereby contaminating surface waters and aquifers.

This paper presents the environmental impact of unconfined slag dumps left over from ancient mining activities in the semiarid Sierra Almagrera region (SE Spain). The risk of abandoned mining areas contaminating soils and groundwater is assessed and long-term contaminant dispersion in the environment is predicted.

2. Geological and metallurgical data

2.1. Study area

The Sierra Almagrera (SA) area (Fig. 1), located 90 km NE of the city of Almería (SE Spain), together with the Iberian Pyrite Belt and the Cartagena mining district, is the oldest metallurgical and mining area of the Iberian Peninsula (Navarro et al., 2004).

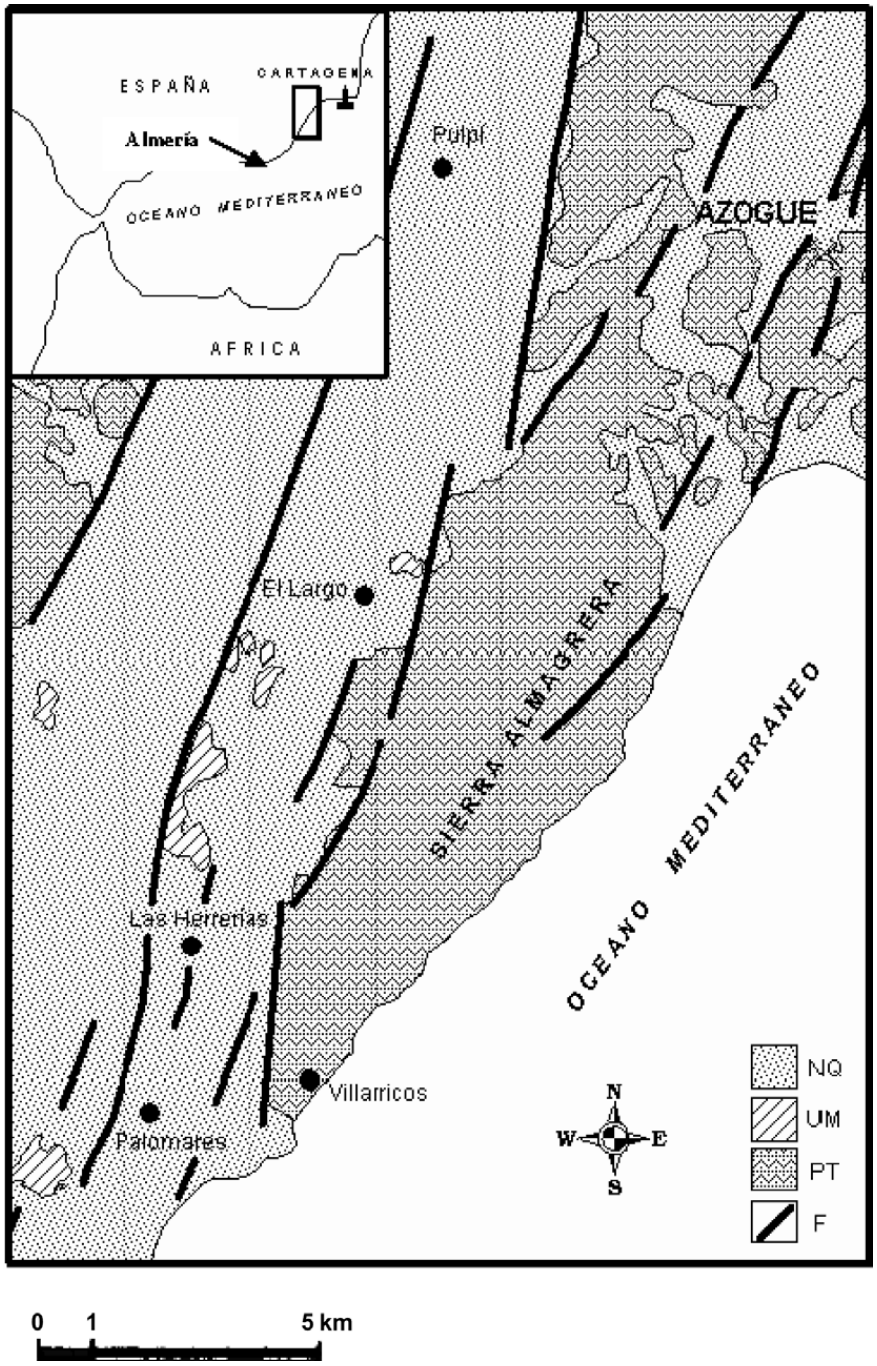

Fig. 1. Geology of the study area. NQ: neogene and quaternary, VM: volcanic-shoshonitic rocks of Miocene age, PT: permian-triassic metamorphic basement, F: main fractures.

The SA mineral deposits are mainly composed of galena, barite, siderite and Ag–Pb sulfosalts. The mineral deposits are located in the Neogene volcanic belt of SE Iberia and were first worked during the 3rd millennium B.C. and later, more intensively, under Carthaginian and Roman occupation, between the 5th century B.C. and the fifth century A.D. Large amounts of mining waste (including smelter slags) were formed in SA and in the major nearby native Ag mine of Herrerías (see Fig. 1).

Modern exploitation began in 1839 with the discovery of the Jaroso vein deposit, that is oriented N–S to N 140 and dips 60–70° E, showing two main branches. The two largest orebodies are 800 m long and 500 m deep, with an average thickness of 4 m (up to 12 m in the upper zone) and an average grade

of 1.2–4.1 kg/t Ag. In the 19th century, about 45 polymetallic veins (0.15–7 m thick) were exploited down to 180 m below sea level, the maximum depth allowed by the available groundwater pumping system (Navarro et al., 1998, 2004).

During the 19th century, the smelting plants located along the Mediterranean coastline of SA had an approximate metal production of 550,000 t of Pb and 512 t of Ag. This production made the SA mining district Spain's main Ag producer from 1841 to 1848 and 1871 to 1880 and its main Pb producer from 1841 to 1868.

During the 20th century, mining activity slowly declined with large periods of inactivity, and the smelting plants were closed in 1915. Selective underground mining (high-grade Pb–Ag veins) was reinitiated in 1945 by the state-owned company MASA (Minas de Almagrera, S.A.) and ceased in 1957, when the exploitation level reached 220 m below sea level and mining costs increased dramatically. From 1967 to 1991, the workings focused on processing low-grade stockpiles, resulting in sand- and silt-sized tailings and one of the largest mining waste accumulations in the area (3,500,000 t) located close to Las Herrerías (Fig. 1), on the western side of Sierra Almagrera. The analysis of the uncontrolled dumping tailings of El Arteal (SA) had high amounts of Ag (29.8 ppm), As (285 ppm), Ba (5.4 wt.%), Cu (57.7 ppm), Pb (2690 ppm), Sb (179 ppm) and Zn (2270 ppm). The oxidation of sulfides and sulfosalts produced the precipitation of less-soluble phases like jarosite ($KFe_3(SO_4)_2(OH)_6$), natrojarosite ($NaFe_3(SO_4)_2(OH)_6$), crystalline oxyhydroxide of Fe (goethite), amorphous ferric hydroxide ($Fe(OH)_3$), clay minerals, anglesite ($PbSO_4$), alunite ($KAl_3(SO_4)_2(OH)_6$) and gypsum ($CaSO_4 \cdot 2H_2O$).

This long mining activity in the SA district (SE, Spain) contaminated groundwater, soil, and fluvial and marine sediments extensively near the old tailings close to the river Almanzora and slag stockpiles in the coastal area.

2.2. Geological setting

The SA mining district is located on the eastern border of the Betic Cordillera, which is the central part of a wide volcanic, tectonic and metallogenic belt that extends to the South from Sierra de Cartagena (Fig. 1). Geologically, the area is composed of metamorphic rocks (schists, phyllites, quartzites and marbles) and volcanic rocks.

The quaternary alluvial and deltaic deposits of the Almanzora river basin unconformably overlie the older materials. These deposits form large terraces in a prograding delta that are 20–30 m thick and are made of sand, gravel and clay. In the coastal area, where this study was carried out, colluvial–alluvial deposits and unconfined slag dumps almost reach the shoreline.

The SA district comprises three main mining areas: Herrerías (stratabound mineralized bodies); Almagrera (N10–40° W veins) and Azogue (veins and breccias associated with a major NE-SW fault). The mineral deposits have been studied in detail by Martínez et al. (1992), Morales (1994), Navarro et al. (1994, 1998) and Viladevall et al. (1999). Preliminary data on the environmental effects of mining activities in the district have also been reported (e.g., Navarro et al., 2000, 2004, 2006b).

The Herrerías mineralization is composed of Fe–Mn oxides, barite, jaspers, native Ag and some sulfides (galena, sphalerite and pyrite). The mineralization in SA is composed of a set of veins enclosed within phyllites and schists that form part of the Permian-Triassic metamorphic basement (Almagrera range). The exploited veins are composed of bournonite, boulangerite, tetrahedrite, galena (Ag-rich), sphalerite, chalcopyrite, pyrite, marcasite, barite, siderite and quartz. Oxidation from supergene alteration produced Fe and Mn oxides, sulfates, carbonates and chlorides. Galena and sulfosalts were the main components of the materials that were processed in local smelters. The oxidized zones were not mined completely, and the mine workings essentially focused on the extraction of sulfosalts (bournonite, boulangerite and tetrahedrite) and sulfides (galena, sphalerite and chalcopyrite).

2.3. Hydrogeological setting

The SA area is located in a semiarid region characterized by a highly irregular hydrological regime, with long periods of dryness and intermittent periods of rain in which the volume of precipitation in a few hours may be greater than the annual average precipitation. The mean precipitation is 285 mm/a with an evapotranspiration of 85–95% of the mean annual precipitation, which indicates that infiltration of rainwater into the soil can be low and that runoff may be very significant during certain periods of the year.

In the coastal area, the impermeable metamorphic rocks of SA are overlain by alluvial–colluvial

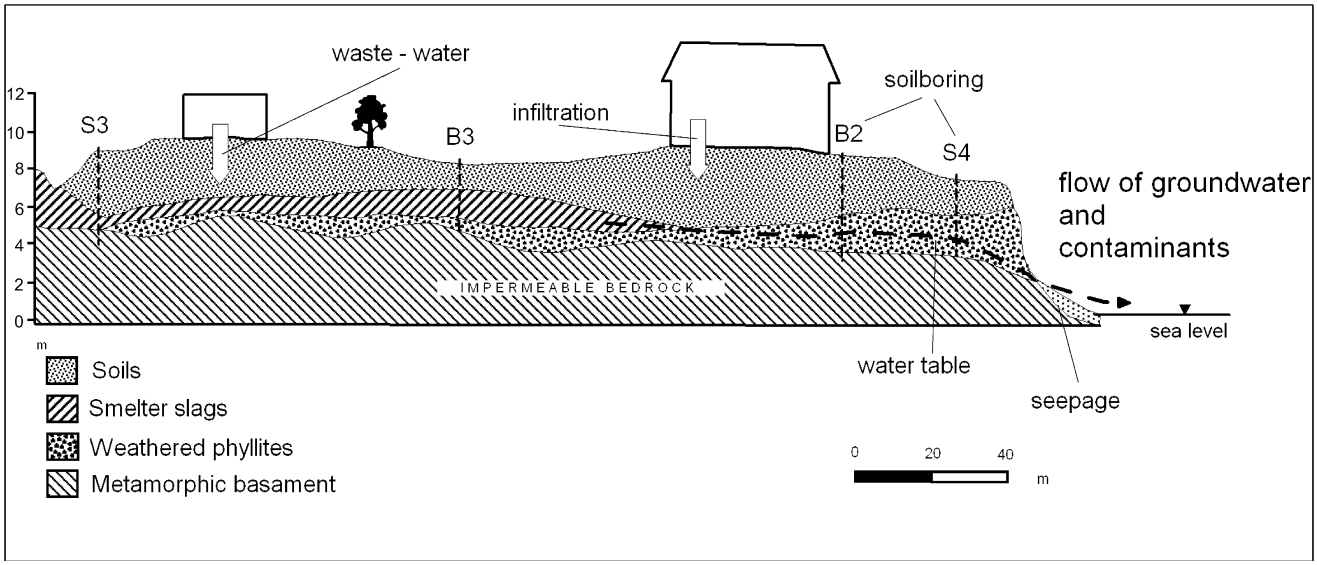

Fig. 2. Profile of the study area and location of the main slag dumps.

sediments and anthropogenic deposits. In the study area, the alluvial–colluvial deposits define an unconfined aquifer associated with low-permeability alluvial and anthropogenic materials that are partially occupied by industrial lands (Fig. 2).

The study area, which is now used for industrial activities, contains a 4–5 m thick unconfined aquifer. The 2 m thick saturated zone is related to levels established by old smelter slags and/or colluvial deposits. The results of pumping tests at a constant flow rate indicate that the aquifer has transmissivities comprised between 20–36 m^2/day and 3–8 m^2/day. The estimated effective porosity values range from 9% to 17% in the higher-transmissivity zone, whereas this parameter could not be evaluated in the lower-transmissivity zone.

Groundwater flows from the higher topographic areas towards the sea. There are two main sources of aquifer recharge: rainwater infiltration and, more importantly, seawater infiltration. Seawater is used in the industrial processes of a major chemical plant built on top of the slags.

2.4. Smelter slags

The slags found around the old smelter sites belong to 17 plants that processed ores from the SA and Herrerías in the 19th and 20th centuries (Fig. 3). The largest slag deposits are found in Las Herrerías, Los Lobos and along the coast. The total amount of accumulated slags is not known because large amounts of them have been used in road construction over the last 50 a. However, based on the district's Pb and Ag production data, an amount greater than 1,500,000 t can be estimated.

At the beginning of the modern mining activity, the metallurgical process in most of the smelters was adapted for the processing of Ag-rich galena (up to 10 kg/t) using cupellation to separate Pb and Ag. However, as Ag grades decreased and international competition with modern foundries increased, cupellation became uneconomic and the smelters began producing only Pb-rich Ag ingots.

This paper examines slags from the Dolores and Santa Ana smelters, which operated from 1850 to 1885. These two sites were chosen because major industrial facilities currently occupy the surface of these slag dumps, which potentially enhances metal mobilization due to sewage infiltration. Around 650,000 t of accumulated slags are located in the study area, which occupies the coastal area between the village of Villaricos and the old Fábrica Nueva smelting site (Fig. 3).

3. Methodology

3.1. Sampling and analysis of soils and slags

The samples for this study were obtained from: (1) unconfined slag dumps around the present-day industrial facilities (samples M1–M10); (2) 8 boreholes (3.5 m deep), which include contaminated soil and slag lenses (soil borings B1–B4 and S1–S4)

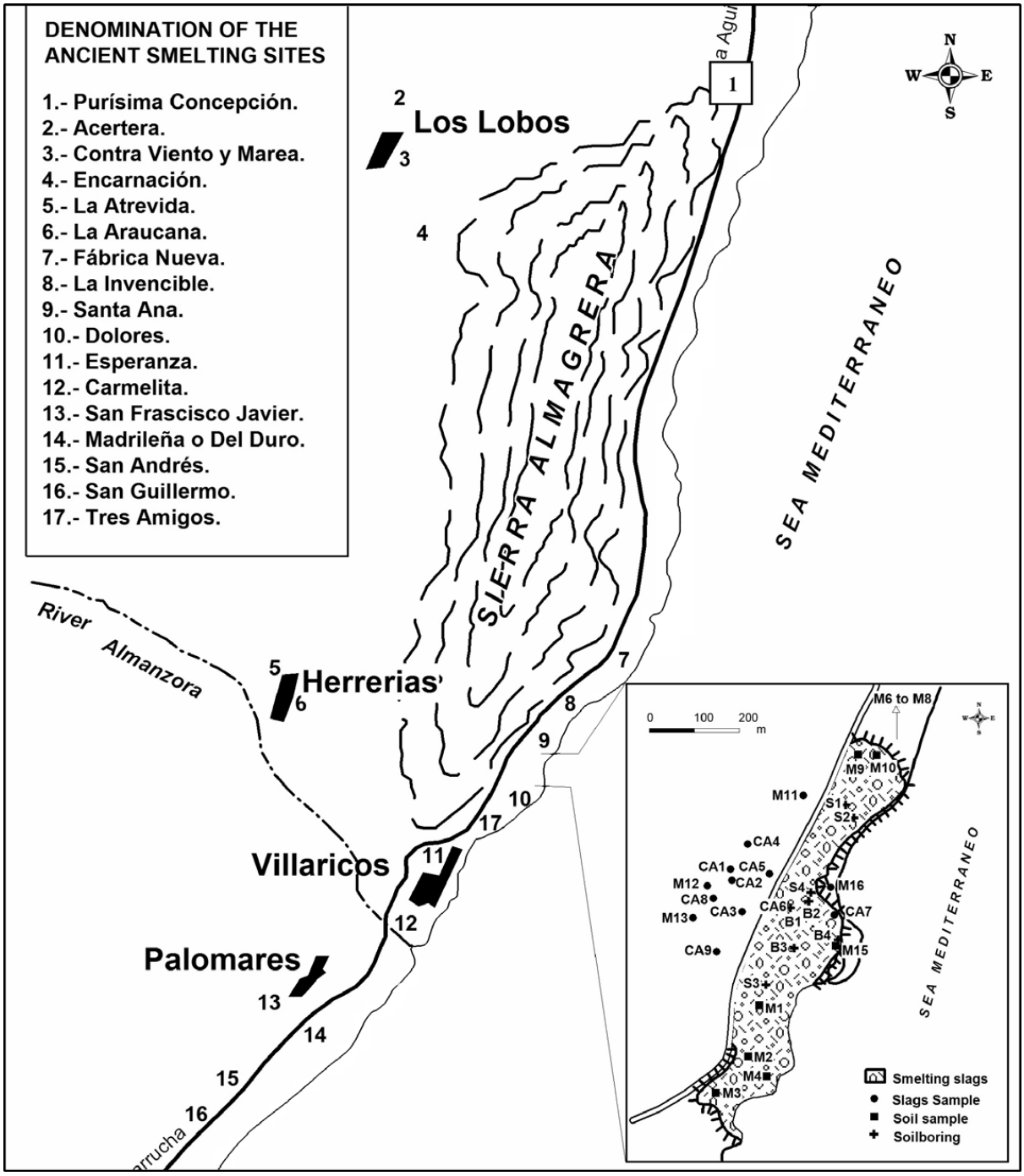

Fig. 3. Location of the old smelting facilities in the Sierra Almagrera area. Situation of soil boreholes and soil–slag samples. M: soils and slags, S: soil boreholes.

underneath the industrial area; and (3) soils from 16 locations sampled in 1996 (samples M-11–M-17) and 2001 (samples CA-1–CA-9) (Fig. 3).

Soil and slag samples were crushed to <10 mesh, quartered, powdered in an agate mortar to <200 mesh, homogenized and packed in sealed plastic bags. Borehole samples were manually collected from drill cores and crushed and powdered similarly to soil and slag samples.

The major and trace element contents of the soil samples were analyzed by inductively coupled plasma atomic-emission spectrometry (ICP-AES), mass spectrometry (ICP-MS) and instrumental neutron activation (INAA) at ACTLABS Laboratories (Canada). A quality control was implemented that included reagent blanks, two duplicate samples and the accuracy was assessed through the analysis of eight reference samples.

The slag samples were studied using transmitted and reflected light microscopy, X-ray diffraction (XRD), scanning electron microscopy (SEM) with an attached energy dispersive system (EDAX), and electron microprobe (EMPA). These techniques allowed the identification of the mineral phases and analysis of the major and trace element contents of the most significant minerals.

3.2. Sampling and analysis of groundwater

Eight groundwater samples (Fig. 4) were collected from eight sampling wells (August 2004) at 4–5 m depth, from a saturated zone of 1–2 m thickness. The piezometer SM has a depth of 40 m, and is completed within the metamorphic basement.

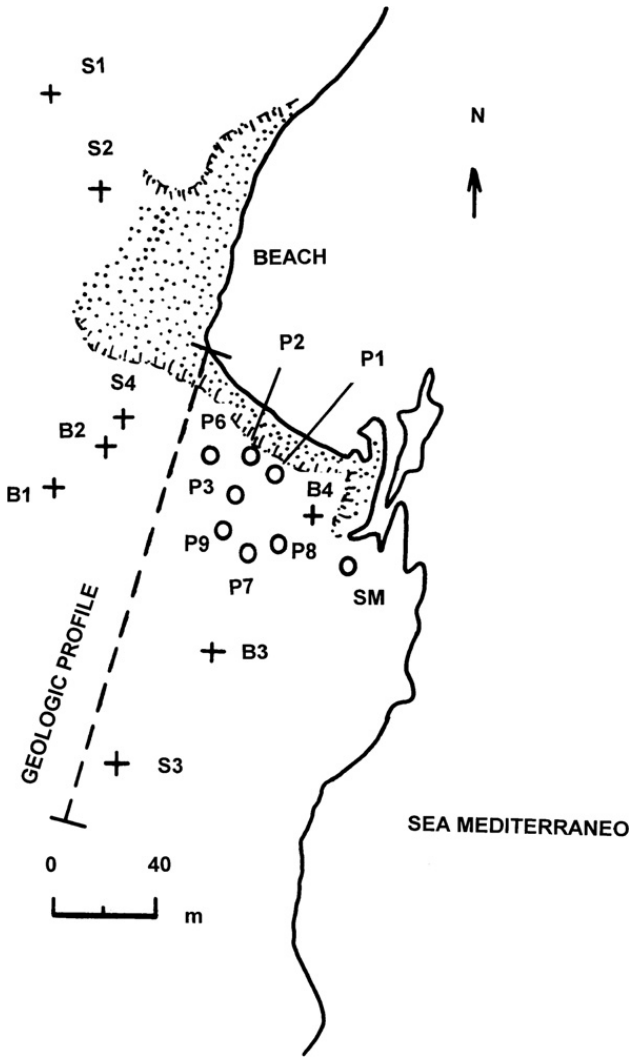

Fig. 4. Detail of the groundwater sampling points. P1–P9: wells, SM: piezometer 40 m depth, S1–S4 and B1–B4: soil boreholes.

The pH, redox potential (Eh; mV), temperature and electrical conductivity (EC; μS/cm), corrected using standard solutions, were measured *in situ* with portable devices (HACH model sensION TM378). The samples were filtered with a cellulose nitrate membrane with a pore size of 0.45 μm. The samples for cation analysis were later acidified to pH < 2.0 by adding ultra-pure HNO_3. The groundwater samples were collected in 500 mL high-density polypropylene bottles, sealed with a double cap and stored in a refrigerator until analysis. The samples were obtained, following purging of each well, using a submersible Grundfos pump, with a flow-rate of 0.5 L/min.

The concentrations of major cations were measured using ICP-AES and the concentrations of minor cations were measured using ICP-MS at the laboratories of the University of Barcelona and ACTLABS. Standard reference material NIST 1640 (ICP-MS) was used to evaluate the accuracy.

3.3. Leaching experiments

A leaching test was performed to evaluate the metal mobility of a mix of smelter slags and potentially contaminated soils. The soil and slag samples used in the elution tests were collected near the main dumping area (Santa Ana-Dolores smelting sites). A column with an internal diameter of 150 mm, a length of 751 mm and an endpiece with a 0.50 μm filter was used. The column was uniformly packed with the reactive material between two thin covers of very low-reactivity polystyrene particles with an equivalent diameter of 2.97 mm. Demineralized water, simulating the effect of the precipitation, was introduced into the column at room temperature by a rain simulator connected to a titration pump, which provided a constant flow rate. Leaching experiments were performed using a stationary flow rate of 2.4 L h^{-1} for 300 min, the equivalent of approximately 6.7 pore volumes. The resulting pore velocity in the experiment was 4.5×10^{-3} m/min, similar to estimated waste water infiltration in the location.

The effluents obtained from the experiments were filtered using cellulose nitrate films with a pore size of 0.45 μm. After determining the pH, temperature, oxidation–reduction potential and electrical conductivity, the samples were stored at 4 °C. The pH was measured potentiometrically and the pH meter was calibrated before each measurement. Conductivity was determined using a conductivity meter

calibrated with an NaCl solution. The oxidation–reduction potential was measured using an ORP meter with a combined Pt electrode.

Samples were then acidified with HCl (pH 1.9) and analyzed using ICP-MS at ACTLABS (Ontario, Canada), for Na, Mg, Al, Si, K, Ca, Sc, Ti, V, Cr, Mn, Fe, Co, Ni, Cu, Zn, Ga, Ge, As, Se, Sr, Y, Zr, Mo, Ru, Pd, Ag, Cd, In, Sn, Sb, Te, Cs, Ba, Pt, Au, Hg, Tl, Pb, Bi and U.

Unacidified samples were stored in low-density polyethylene (LDPE) bottles and Cl, HCO_3, CO_3, NO_3 and SO_4 were analyzed using ion chromatography and other common methods (APHA, 1989). The accuracy of the results was assessed by examining blanks and the standard reference material NIST 1640 (ICP-MS), and by performing charge-balance calculations for all samples. The results of the charge-balance calculations indicate an error of between 1% and 25%.

Hydrogeochemical analyses of leachates were performed by using the PHREEQC (Parkhurst and Appelo, 1999) numerical code (version 2.10.03) to evaluate the speciation of dissolved constituents and calculate the saturation state of the effluents. The Minteq thermodynamic database was used for the chemical equilibrium calculations.

4. Results and discussion

4.1. Mineralogy of slags

The slags are composed of various silicate, sulfate, oxide, sulfide and metallic phases accompanied by secondary minerals resulting from weathering. No glassy phases were observed. The primary phases include quartz, fayalite, barite, melilite, celsian, pyrrhotite, magnetite, galena and Zn–Pb–Fe alloys. Jarosite–natrojarosite, cotunnite, cerussite,

Table 1
Chemical analyses by microprobe of mineral phases identified in slags (wt.%)

	Na_2O	MgO	Al_2O_3	SiO_2	SO_3	Cl_2O	K_2O	CaO	TiO_2	Cr_2O_3	MnO	FeO	NiO	CuO	ZnO	SrO	BaO	PbO	Sum
Olivine																			
Average	**0.05**	**3.11**	**0.01**	**30.2**	**0.00**	**0.01**	**0.00**	**1.82**	**0.06**	**0.03**	**3.35**	**59.2**	**0.02**	**0.01**	**1.34**	**0.01**	**0.22**	**0.03**	**99.5**
Max	0.11	4.91	0.02	30.9	0.03	0.13	0.02	2.36	0.14	0.05	3.68	61.2	0.05	0.04	1.51	0.05	0.38	0.18	
Min	<0.01	1.71	<0.01	29.4	<0.01	<0.01	<0.01	1.2	0.01	0.01	3.1	57.8	<0.01	<0.01	1.27	<0.01	<0.01	<0.01	$n = 13$
Celsian																			
Average	**0.45**	**0.05**	**23.4**	**38.5**	**0.13**	**0.07**	**3.08**	**0.21**	**0.03**	**0.01**	**0.06**	**1.78**	**0.02**	**0.04**	**1.52**	**2.54**	**21.2**	**0.31**	**93.4**
Max	0.54	0.09	23.7	39.8	0.54	0.45	3.33	0.54	0.07	0.03	0.08	2.89	0.06	0.03	2.52	3.22	30.5	0.42	
Min	0.34	<0.01	22.4	37.1	<0.01	<0.01	2.65	0.05	<0.01	<0.01	0.03	0.52	<0.01	<0.01	0.15	0.51	17.8	0.1	$n = 9$
Melilite																			
Average	**2.32**	**0.07**	**2.58**	**30.6**	**1.54**	**1.38**	**0.80**	**10.4**	**0.97**	**0.02**	**0.70**	**21.2**	**0.03**	**0.01**	**2.09**	**2.77**	**19.4**	**0.22**	**97.1**
Max	2.9	0.1	3.04	31.1	1.84	1.64	0.85	10.6	1.17	0.04	0.81	21.9	0.08	0.03	2.52	3.22	21.2	0.42	
Min	2.08	0.04	2.18	29.7	1.17	1.13	0.73	10.1	0.64	<0.01	0.57	19.6	0.01	<0.01	1.52	2.54	17.8	0.02	$n = 6$

	S	Cl	Mn	Fe	Co	Ni	Cu	Zn	Ge	As	Ag	Sb	Ba	Pb	Sum
Pyrrhotite															
Average	**36.9**	**0.03**	**0.14**	**60.5**	**0.08**	**0.03**	**0.61**	**0.07**	**0.02**	**0.16**	**0.02**	**0.00**	**0.23**	**0.94**	**99.7**
Max	37.6	0.06	0.17	61.3	0.12	0.06	0.87	0.16	0.03	0.29	0.06	0.01	0.24	3.21	
Min	35.7	<0.01	0.01	59.5	0.06	<0.01	0.2	0.03	<0.01	<0.01	<0.01	<0.01	0.03	0.12	$n = 4$
Cotunnite															
Average	0.32	19.2	0.09	1.37	0.01	0.02	0.04	0.24	0.06	0.39	0.00	0.06	0.31	78.1	100.2
Max	0.48	21.8	0.12	2.53	0.04	0.05	0.07	0.33	0.11	0.47	0.02	0.26	0.7	80.7	
Min	0.01	15.6	0.06	0.51	<0.01	<0.01	<0.01	0.15	<0.01	0.32	<0.01	<0.01	0.13	75.8	$n = 5$
Galena															
Average	**12.2**	**1.11**	**0.07**	**3.88**	**0.03**	**0.03**	**0.30**	**0.32**	**0.02**	**0.06**	**0.05**	**0.01**	**0.35**	**78.4**	**96.8**
Max	13.0	1.82	0.08	7.07	0.04	0.05	0.31	0.55	0.03	0.1	0.08	0.01	0.07	84.9	
Min	11.4	0.4	0.06	0.68	0.02	<0.01	0.28	0.09	<0.01	0.01	0.02	<0.01	<0.01	71.9	$n = 2$
Magnetite															
	0.01	**0.01**	**0.29**	**59.1**	**0.06**	**<0.01**	**<0.01**	**0.77**	**0.04**	**<0.01**	**0.02**	**<0.01**	**0.07**	**0.07**	**60.4**
															$n = 1$

Structural formula of melilite: $Ca_{0.7}Ba_{0.4}Na_{0.3}Sr_{0.1}Fe_{1.1}Zn_{0.1}Al_{0.1}Si_2O_7 \times (Cl_{0.1},S_{0.1},OH_{0.1})$, if total Fe is considered Fe(II), but if total Fe is considered Fe(III), then the structural formula is $Ca_{0.7}Ba_{0.4}Na_{0.3}Sr_{0.1}Zn_{0.1}Fe^{3+}_{1.1}Al_{0.1}Si_2O_7$ and the sum of oxides averages more than 99%. *n*: Number of samples.

goethite, ferrihydrite, chalcanthite, copiapite, goslarite, halotrichite and szomolnokite were found as secondary phases. Anglesite and gypsum were also detected in minor quantities. Table 1 shows a quantitative analysis of certain representative minerals.

Sierra Almagrera slags show textures composed of a matrix of silicate crystals (olivine, celsian and melilite). Olivine occurs as short prismatic crystals up to 5 mm in length, whereas melilite and celsian appear as elongated blades (Fig. 5). Sulfides, especially pyrrhotite, occur as rounded blebs 1–20 μm in diameter distributed throughout the samples (Fig. 5). Minor phases (cotunnite, magnetite, goethite and Zn–Pb–Fe alloys) appear scattered throughout the matrix and along silicate grain boundaries.

Table 1 shows the olivine composition in the slags. Olivines are Fe-rich (Fa_{82}) with MnO and MgO content of up to 3.7 and 4.9 wt.%, respectively. Amounts of up to 1.5 wt.% ZnO and 2.4 wt.% CaO were detected (see Table 1). These Zn and Ca concentrations are similar to those reported in olivine-bearing slags from the Vermont Cu belt by Piatak et al. (2004).

Celsian and melilite are two other major silicate phases. The celsian contains up to 30.5 wt.% BaO and reflects the presence of abundant barite in the ores. Iron content is relatively high, up to 2.9 wt.% FeO_T. Lead (up to 0.4 wt.% PbO) and Zn (up to 2.5 wt.% ZnO) were also found in this mineral (see Table 1). The melilites are Ba–Fe-rich (up to 21 and 22 wt.% BaO and FeO_T, respectively) and Ca-poor compared to natural occurrences (Deer et al., 1975). They also contain S, Cl and Zn (up to 2.5 wt.% ZnO).

Galena (PbS), pyrrhotite ($Fe_{(1-x)}S$), cotunnite ($PbCl_2$), Fe oxides (magnetite and goethite) and sulfates are the most abundant metal-bearing phases. They are volumetrically minor slag components but may be significant sources of metal to the environment. Pyrrhotite blebs contain small amounts of Zn, Pb and As and, due to their reactivity, are a potential source of metal contamination. Cotunnite is a common secondary slag phase whose origin is not well understood. This secondary phase, formed by the reaction of Pb-bearing minerals (galena) with Cl^-, might be formed by the infiltration of high-Cl effluent, also, with wastewater of low salinity, from the chemical plants built on top of the slags, which use seawater in the refrigeration processes. However, because SA slags were dumped along the coast, direct sea spray could be an additional Cl^- source.

The presence of other soluble and less-soluble secondary phases (Fe–Cu sulfates such as chalcanthite, copiapite, halotrichite and szomolnokite) is especially important in the mobilization of metals. During rainy periods, the dissolution of secondary sulfates may cause the formation of acid effluents that could either affect surface waters or infiltrate

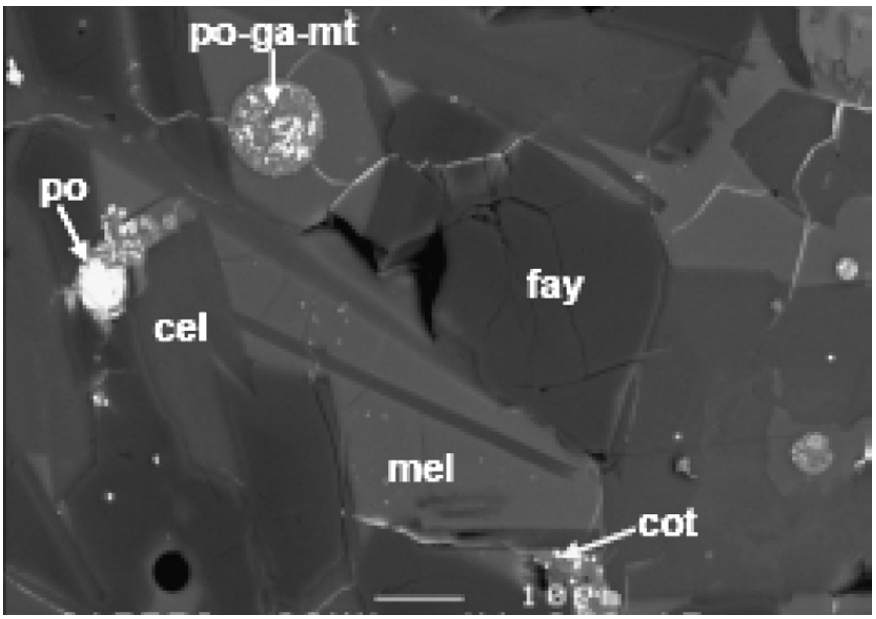

Fig. 5. Backscattered electron photomicrograph of a polished section of a smelter slag. cot: cotunnite; fay: fayalite; mel: melilite; po: pyrrhotite; ga: galena; mt: magnetite; cel: celsian.

into soils and cause seasonal contaminating pulses (Bigham and Nordstrom, 2000; Jambor et al., 2000). In semiarid environments like the study area, the role of the secondary phases accumulated in soils and mining residues during dry periods is very significant. In fact, the mobilization of Cu, Pb and Zn from the tailings dumped near the Almanzora River, was partially explained by the presence of langite, melanterite, brochantite, chalcanthite, anglesite, plumbojarosite, goslarite and other secondary phases that formed as a result of the supergene alteration of metallic sulfides (Navarro et al., 2004).

4.2. Chemical composition of soils and slags

The SA slag dumps contain high concentrations of metals and metalloids: Ag (<5–180 ppm), As (12–750 ppm), Cu (45–183 ppm), Fe (83.2–29.8 wt.%), Pb (511–2150 ppm), Sb (22–620 ppm) and Zn (639–8600 ppm). Barium concentrations are also high (0.4–19.0 wt.%), due to the mineralogical composition of the vein ores (barite is present). Table 2 shows the metal composition of the slags from surface samples and samples of a soil profile from site S-2.

Compared to the slags, the soil samples show higher concentrations of As, Ba, Cu, Pb, Sb and Zn, but lower concentrations of Ag (Table 3). Soil contamination of As, Ba, Pb, Sb and Zn is probably related to the weathering of smelter slags, although some of this contamination might also be due to emissions from the old smelters, which had been active for at least 30 a. However, only four metals and metalloids (As, Hg, Pb and Sb) exceed the soil remediation intervention values, according to the internationally known Netherlands regulations (Ministry of Housing Spatial Planning and Environment, 2000).

Drill cores in the soils allowed the evaluation of the distribution of metals with depth and determination of the chemical composition of the slag layers (Figs. 6 and 7). Some metal concentrations tend to decrease with depth, such as Cu, Mn, Pb and Zn in soil boring S-1 (Fig. 6). In addition, because reducing and slightly acidic conditions prevail in most of the groundwater sampled during this study, the dissolution of Fe oxyhydroxides could mobilize any adsorbed Zn.

The formation of Fe oxyhydroxides might be related to the oxidation of sulfide-bearing minerals (especially pyrrhotite) in the slags. This process

Table 2
Composition of slags from surface samples and samples from a soil profile at site S2

Element	Au (ppb)	Ag (ppm)	As (ppm)	Ba (%)	Br (ppm)	Co (ppm)	Cr (ppm)	Cs (ppm)	Fe (%)	Hg (ppm)	Mo (ppm)	Na (%)	Ni (ppm)	Sb (ppm)	Zn (ppm)	Cu (ppm)	Pb (ppm)	Mn (ppm)	Sr (ppm)	Cd (ppm)	V (ppm)	Ca (%)	P (%)	Mg (%)
M-1	<5	49	440	0.88	8	29	97	11	17	<1	30	0.62	210	370	1000	ND	ND	ND	ND	ND	ND	ND	ND	ND
M-2	<5	130	540	3.0	23	33	55	7	20.6	<1	29	0.58	<50	620	2560	ND	ND	ND	ND	ND	ND	ND	ND	ND
M-3	<5	140	180	19.0	<1	16	<10	<2	14.9	<1	<5	0.12	<50	500	2600	ND	ND	ND	ND	ND	ND	ND	ND	ND
M-4	9	12	170	5.6	23	36	50	4	25.4	<1	19	0.48	<50	80	6900	ND	ND	ND	ND	ND	ND	ND	ND	ND
M-5	<5	20	140	7.9	17	33	57	<2	29.8	<1	50	0.33	<50	76	8600	ND	ND	ND	ND	ND	ND	ND	ND	ND
M-6	<5	<5	100	0.44	13	83	210	7	8.55	<1	23	0.5	<50	25	701	ND	ND	ND	ND	ND	ND	ND	ND	ND
M-7	12	180	750	2.8	<1	8	53	4	21.9	<1	81	0.21	<50	320	2480	ND	ND	ND	ND	ND	ND	ND	ND	ND
M-8	<5	170	340	2.5	6	14	50	4	18.3	<1	16	0.23	<50	390	3480	ND	ND	ND	ND	ND	ND	ND	ND	ND
M-9	12	110	140	7.0	12	26	85	12	16.4	<1	93	0.4	<50	330	3670	ND	ND	ND	ND	ND	ND	ND	ND	ND
M-10	<5	64	87	4.5	12	17	81	11	15.3	<1	23	0.52	<50	300	2100	ND	ND	ND	ND	ND	ND	ND	ND	ND
S2																								
0–0.6 m	<2	<5	12	0.78	32	6	77	3	3.22	29	15	1.62	30	22	639	45	511	1210	324	1.2	51	2.46	0.527	0.62
0.6–1 m	4	19	43	1.50	9.7	17	98	10	8.48	3	4	0.89	49	67	1020	158	1400	3810	594	0.9	134	1.39	0.173	0.76
1–2.2 m	<2	42	36	4.30	7.7	16	85	8	14	<1	18	0.8	44	150	1830	183	2090	9190	1330	0.5	122	1.56	0.139	0.67
2.2–3 m	2	38	29	5.80	5.4	11	70	7	13.4	<1	15	0.73	37	150	2280	176	2150	9950	1830	<0.5	121	1.91	0.125	0.67

Au to Sb analyzed by INAA, Mo to Mg by ICP-MS.
ND: not analyzed.

Table 3
Composition of soils sampled

Elements	Au	As	Ba	Br	Co	Cr	Cs	Fe	Hg	Mo	Na	Ni	Rb	Sb	Zn	Ag	Cd	Cu	Mn	Pb	Mg	P	Sr	V	S
	(ppb)	(ppm)	(ppm)	(ppm)	(ppm)	(ppm)	(ppm)	(%)	(ppm)	(ppm)	(%)	(ppm)	(ppm)	(ppm)	(ppm)	(ppm)	(ppm)	(ppm)	(ppm)	(ppm)	(%)	(%)	(ppm)	(ppm)	(%)
M-11	8	100	3100	7	17	120	8	6.51	<1	10	0.94	<50	150	60	850	<5	ND	ND	ND	ND	ND	ND	ND	ND	ND
M-12	12	69	750	14	15	130	10	6.01	<1	7	0.79	210	150	19	335	<5	ND	ND	ND	ND	ND	ND	ND	ND	ND
M-13	<5	110	1800	170	16	110	9	5.31	5	8	1.91	<50	140	32	400	<5	ND	ND	ND	ND	ND	ND	ND	ND	ND
M-14	6	27	770	11	11	91	7	4.52	<1	<5	0.84	<50	91	7.3	313	<5	ND	ND	ND	ND	ND	ND	ND	ND	ND
M-15	<5	20	1200	23	11	170	4	3.7	<1	17	1.08	160	57	8.1	1300	<5	ND	ND	ND	ND	ND	ND	ND	ND	ND
M-16	<5	51	4200	11	12	62	4	5.67	<1	6	0.44	100	59	28	560	<5	ND	ND	ND	ND	ND	ND	ND	ND	ND
M-17	13	100	2800	43	16	100	9	5.62	8	15	1.01	<50	98	39	530	<5	ND	ND	ND	ND	ND	ND	ND	ND	ND
CA-1	<2	21.8	450	3.9	11	52	5	3.75	42	4	0.22	30	62	4.8	349	<0.3	0.8	22	311	249	0.34	0.07	71	52	0.23
CA-2	<2	546	960	10.7	19	79	11	4.69	<1	5	0.59	39	117	126	118	<0.3	8.4	22	390	1892	0.71	0.05	302	115	3.28
CA-3	5	553	1200	174	18	87	11	5.35	<1	6	0.99	43	164	108	158	0.4	1.9	37	407	7177	1.01	0.20	212	135	1.79
CA-4	<2	33.7	800	13.8	23	117	12	5.5	<1	6	0.68	56	151	10	129	<0.3	0.3	28	606	132	0.94	0.13	139	150	0.15
CA-5	<2	35.5	890	6.6	24	184	22	5.91	<1	13	0.76	79	145	13	272	<0.3	0.8	36	551	140	1.50	0.08	193	164	0.09
CA-6	<2	171	820	8.6	19	110	12	6.22	<1	7	0.77	46	170	33.5	144	0.4	3.1	33	442	1554	1.31	0.07	148	151	0.41
CA-7	<2	46.3	2600	15.6	15	79	9	5.68	<1	4	0.77	46	80	30.3	324	3.2	0.9	60	825	1176	1.38	0.13	430	130	1.18
CA-8	2	95.8	670	<0.5	30	103	15	5.41	<1	5	0.65	64	112	23.8	195	<0.3	6.6	24	580	435	0.87	0.08	138	153	0.05
CA-9	<2	81.7	800	<0.5	35	111	11	6.34	<1	8	0.75	64	157	15.2	170	<0.3	2.2	38	741	125	1.34	0.08	144	163	0.03

Au to Sb analyzed by INAA, Ag to S analyzed by ICP-MS.
ND: not analyzed.

may lead to the precipitation of poorly-crystalline Fe hydroxide phases such as ferrihydrite or goethite (FeOOH) and Fe sulfates such as schwertmannite [$Fe_8O_8(SO_4)(OH)_6$], depending on kinetic factors, Fe^{3+}, SO_4^{2-} and HCO_3^- concentrations and, especially, pH. Thus, the activity of Fe is controlled by ferrihydrite and schwertmannite for pHs between 4.5 and 6.5 and by ferrihydrite when pH > 6.5 (Balistrieri et al., 2002).

4.3. Chemical composition of groundwater

Groundwater samples collected during this study have high Cu, Fe, Mn, Pb, Zn and As contents (Table 4), reaching up to 0.64 mg/L Cu, 40 mg/L Fe, 0.6 mg/L Mn, 7.6 mg/L Zn, 5.1 mg/L Pb and 19 μg/L As. These concentrations suggest that metals are mobilized from the surrounding smelter slags and contaminated soils.

However, the Ag and Sb contents are low, as in the results obtained in the leaching experiments of tailings from this area (Navarro et al., 2004). In fact, Ag is almost immobile at pH > 4 (Lindsay, 1979) and is easily absorbed by clay minerals, Fe and Mn oxides and hydroxides, and organic matter, which are quite abundant in this aquifer.

Probably due to the partial infiltration of seawater used by industrial facilities, the groundwater is highly saline (electrical conductivity: 6850–70,300 μS/cm), slightly acidic to near neutral, and is reducing or slightly oxidizing (Table 4).

The high Fe concentration is consistent with the pH-Eh values of the groundwater. A weak positive correlation between dissolved Fe and reducing Eh was seen (Fig. 8). There is an inverse relationship between pH and Fe content (Fig. 9), as found in most aquifers contaminated by mining waste (Seal and Hammarstrom, 2003) where higher Fe concentrations are found in more acidic waters.

The main source of Fe may be the oxidation of pyrrhotite by O_2, that may release Fe(II) and SO_4 to pore water and groundwater through the following reaction:

$$Fe_{(1-x)}S_{(s)} + (2 - x/2)O_2(g) + H_2O = (1 - x)Fe^{2+} + SO_4^{2-} + 2xH^+$$

Calculations using PHREEQC for groundwater speciation (Table 5) show that the most abundant species of Fe are Fe^{2+} and $FeSO_4$. Likewise, the saturation index indicates that ferrihydrite, jarosite, natrojarosite and melanterite are clearly

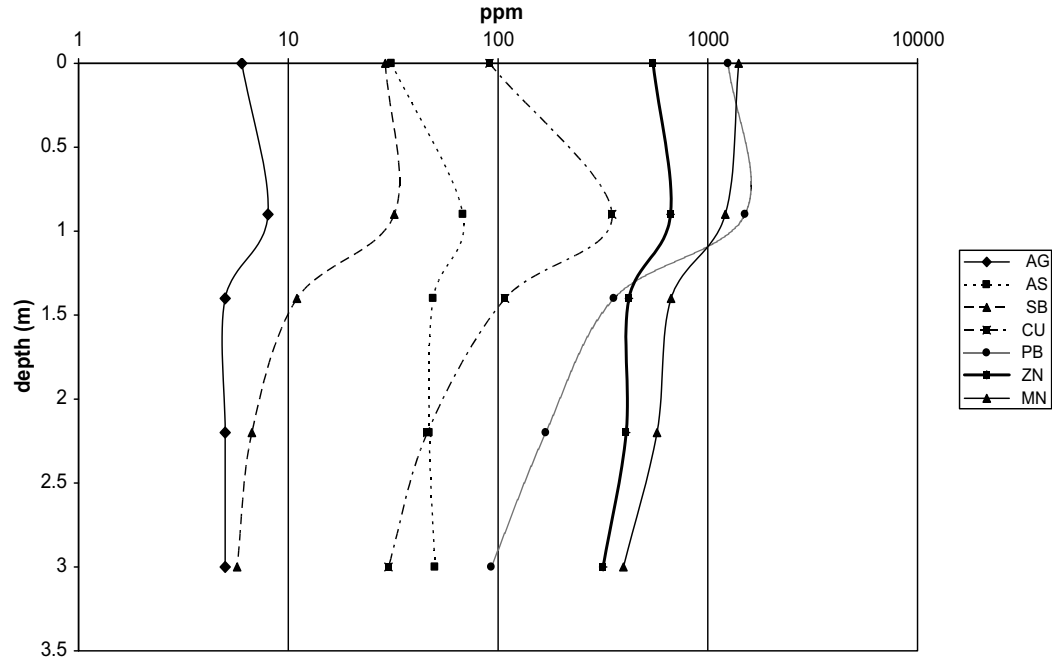

Fig. 6. Ag, As, Cu, Mn, Pb, Sb and Zn distribution in drill core S-1. Values in ppm.

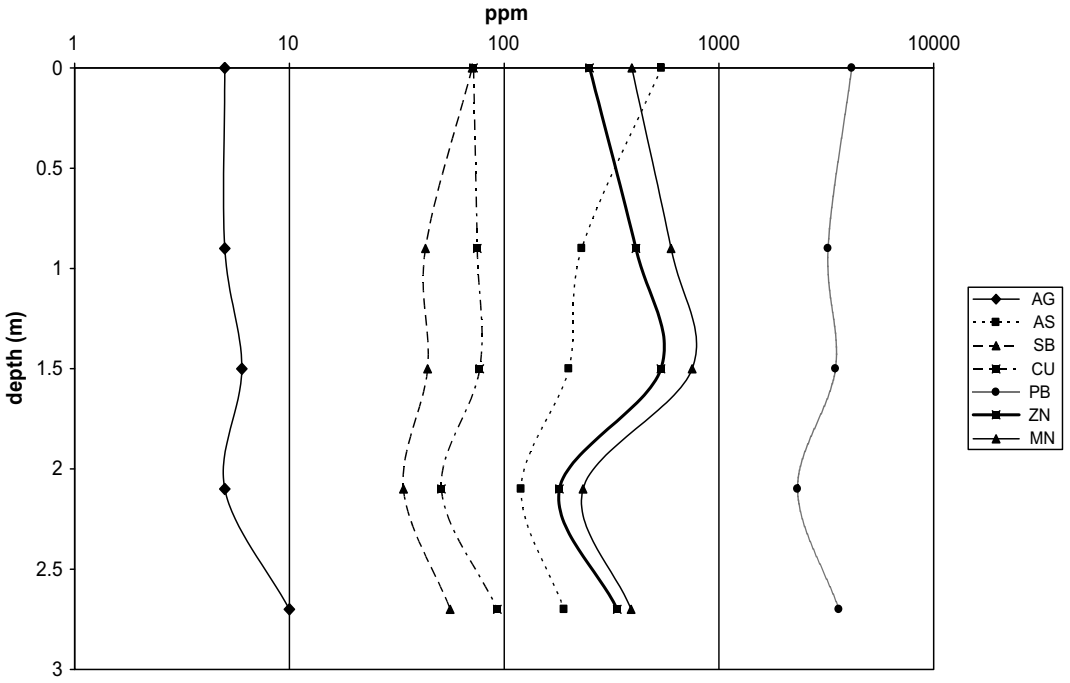

Fig. 7. Ag, As, Cu, Mn, Pb, Sb and Zn distribution in drill core S-3. Values in ppm.

undersaturated, suggesting the possibility of dissolution (Table 6).

In contrast, goethite is slightly undersaturated (Table 6) or saturated (sample SM), indicating goethite as a mineral phase which controls the solubility of Fe. Besides, the mineral phase $Fe(OH)_{2.7}Cl_{0.3}$ is also saturated except in sample P3. The predominant secondary Fe phases within the unconfined slags are goethite, ferrihydrite, jarosite and soluble Fe-sulfates, which occur as interstitial cements, and since ferrihydrite, jarosite and melanterite are clearly undersaturated in groundwater, their disso-

Table 4
Composition of contaminated groundwater in the study area

Well	Eh	pH	Ag	Al	As	Cd	Cu	Fe	Mn	Ni	Pb	Sb	Zn	K	Mg	Na	SO_4
P1	−0.1	6.3	<0.02	<0.2	19	<0.02	<40	40.1	40	<0.25	40	<4	200	209	680	10,200	2660
P2	0.04	6.9	<0.02	0.01	6	<0.02	10	0.6	10	1.2	2	<4	313	24.9	57	755	241
P3	−0.08	5.8	<0.02	<0.2	15	<0.02	20	3.9	20	<0.25	40	<4	500	225	831	9890	2670
P6	0.03	5.8	<0.02	<0.02	7	<0.02	24	0.9	20	<0.25	4	16	78	105	283	3220	835
P7	−0.02	5.6	<0.02	0.52	7	<0.02	40	2.5	40	<0.25	40	<4	380	415	1288	11,900	1410
P8	−0.2	7.1	<0.02	<0.02	8	<0.02	18	1.6	18	<0.25	4	<4	74	261	523	5250	1380
P9	−0.1	5.6	<0.02	4.22	1	<0.02	40	13.2	40	<0.25	80	<4	7680	304	1007	9710	1120
SM	0.06	6.8	<0.02	0.32	1	<0.02	640	0.4	640	<0.25	5140	60	1520	404	1040	12,300	2070

Concentrations determined by ICP-AES and ICP-MS and reported in mg/L, except for Ag, As, Cd, Cu, Mn, Pb, Sb and Zn (μg/L). Eh reported in V. SM: piezometer of 40 m depth.

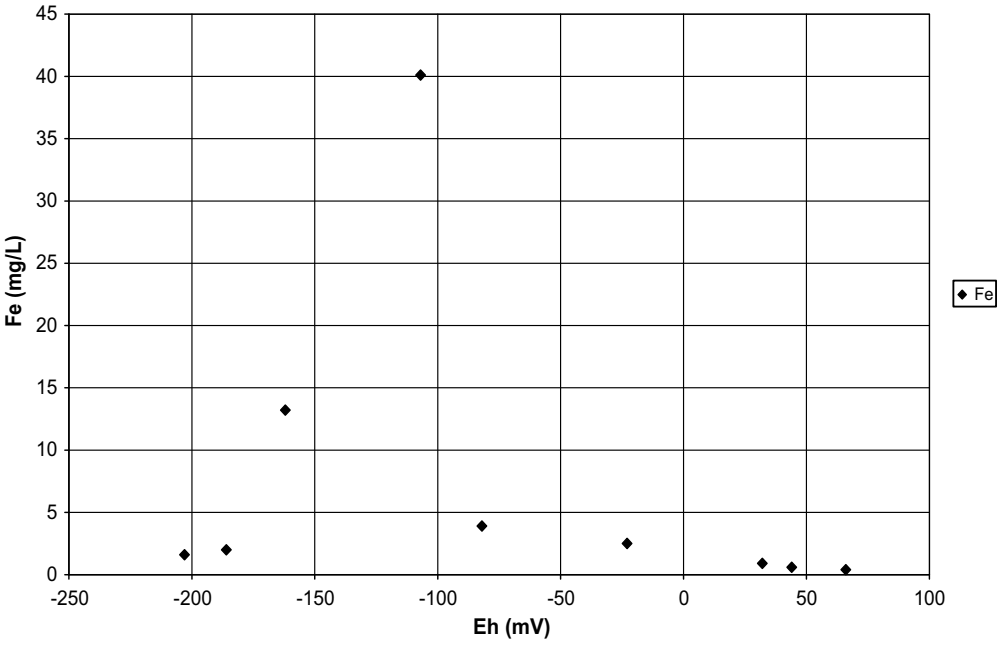

Fig. 8. Relationship between Eh and dissolved Fe in contaminated groundwater.

lution may explain, with the oxidation of the pyrrhotite, the high contents of the Fe detected in groundwater.

Lead concentration reaches up to 5.14 mg/L in the most oxidizing and saline sample (Fig. 10). At the pH conditions of the aquifer (5.6–7.2), geochemical modeling indicates that the Pb speciation (Table 5) may be dominated by $PbCl^+$ and $PbCO_3$ (aq). Therefore, Pb concentration could be controlled by several of the mineral phases recognized in the mineralogical study such as cerussite ($PbCO_3$) and cotunnite ($PbCl_2$), which are undersaturated in groundwater samples (Table 6). Thus, the high salinity of the groundwater might explain the mobility of Pb, because like other heavy metals, it tends to form Cl complexes such as $PbCl^+$ and $PbCl_2$, which are relatively soluble.

Zinc is the metal with the highest concentrations in groundwater, reaching values of up to 7.68 mg/L (Fig. 11). Zinc mobility in near-neutral environments is limited because it is readily adsorbed by oxides, hydroxides and aluminosilicates. High Zn concentrations in groundwater and soils are usually related to ferrihydrite desorption or dissolution processes (Jurjovec et al., 2002). Under the pH-Eh conditions of the aquifer, the Zn speciation may be dominated by Zn^{2+} and $ZnHCO_3^+$ (Table 5). The secondary phase mineral goslarite ($ZnSO_4 \cdot 7H_2O$) is clearly undersaturated (Table 6). Copper concentrations reach up to 0.64 mg/L, which indicates that this metal is highly soluble in saline environments with a pH below neutral.

The As content in the groundwater reaches 19 μg/L, but ranges from 1 to 8 μg/L in most of

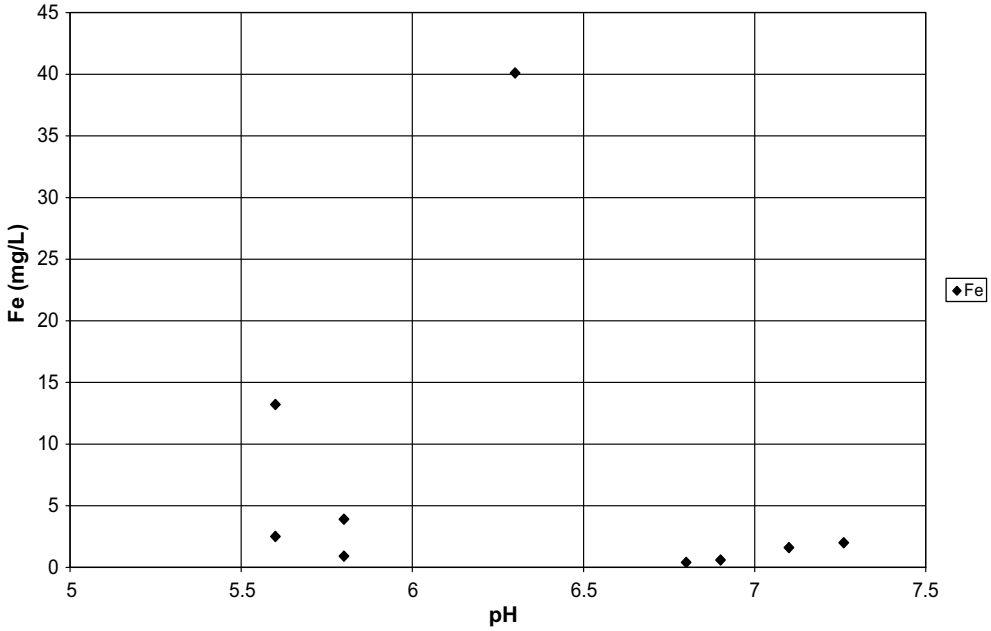

Fig. 9. Relationship between pH and dissolved Fe in contaminated groundwater.

Table 5
Distribution of species for groundwater and leachate D1

Species	P1	P3	P6	P8	SM	D1
As						
H_3AsO_3	2.56×10^{-7}	2.03×10^{-7}	9.32×10^{-8}	1.06×10^{-7}	2.74×10^{-10}	7.06×10^{-11}
$H_2AsO_3^-$	4.60×10^{-10}	1.16×10^{-10}	4.82×10^{-11}	1.17×10^{-9}	1.59×10^{-12}	2.94×10^{-14}
Fe						
Fe^{2+}	6.51×10^{-4}	6.41×10^{-5}	1.47×10^{-5}	2.65×10^{-5}	6.83×10^{-6}	1.20×10^{-4}
$FeSO_4$	7.60×10^{-5}	6.81×10^{-6}	1.39×10^{-6}	2.30×10^{-6}	4.65×10^{-7}	6.16×10^{-5}
$FeOH^+$	1.51×10^{-7}	4.62×10^{-9}	1.32×10^{-9}	4.14×10^{-8}	4.75×10^{-9}	5.58×10^{-9}
Pb						
$PbCl^+$	6.02×10^{-8}	8.41×10^{-8}	7.82×10^{-9}	2.31×10^{-9}	1.03×10^{-5}	4.29×10^{-6}
$PbCO_3$	5.19×10^{-8}	1.58×10^{-8}	1.32×10^{-9}	1.35×10^{-8}	6.42×10^{-6}	1.34×10^{-9}
$PbHCO_3^+$	3.60×10^{-8}	3.51×10^{-8}	2.65×10^{-9}	1.45×10^{-9}	1.44×10^{-6}	4.32×10^{-9}
Pb^{2+}	2.38×10^{-8}	2.77×10^{-8}	5.07×10^{-9}	7.58×10^{-10}	2.73×10^{-6}	1.00×10^{-6}
$PbCl_2$	1.01×10^{-8}	1.68×10^{-8}	1.16×10^{-10}	4.83×10^{-10}	2.49×10^{-6}	1.05×10^{-6}
Zn						
Zn^{2+}	1.93×10^{-6}	4.96×10^{-6}	8.86×10^{-7}	5.82×10^{-7}	1.59×10^{-5}	1.74×10^{-5}
$ZnHCO_3^+$	4.13×10^{-7}	8.59×10^{-7}	7.81×10^{-8}	1.72×10^{-7}	1.05×10^{-6}	1.17×10^{-5}[a]

Data calculated using PHREEQC and database MINTEQ. Values in molality.
[a] $ZnSO_4$.

the samples. These concentrations are similar to those obtained in column-leaching experiments with tailings (Navarro et al., 2004) and indicate a low mobility of the metalloid. Arsenic can be mobilized in reducing or oxidizing conditions at pH values of 6.5–8.5. In natural waters, As may be present as As(III), As(V) or linked to organic forms after industrial contamination processes (Smedley and Kinniburgh, 2002). In contrast to most metallic cations, a pH increase causes the anionic forms of As to be desorbed from soils or solid phases in the saturated zone of the aquifers and As becomes relatively mobile under reducing conditions. Under oxidizing conditions, the dominant species at pH < 6.9 is $H_2AsO_4^-$, whereas $H_3AsO_3^0$ dominates at alkaline pH. In the studied groundwaters, where

Table 6
Calculated saturation index for groundwater and lixiviate D1

Phase mineral	P1	P3	P6	P8	SM	D1
Iron oxy-hydroxides						
$Fe(OH)_3$	−4.63	−6.72	−5.29	−5.21	−2.22	−1.45
Goethite	−0.23	−2.32	−0.90	−0.81	2.17	−2.95
$Fe(OH)_{2.7}Cl_{0.3}$	1.18	−0.74	0.59	0.38	3.48	4.61
Sulfate minerals						
Jarosite	−10.8	−15.6	−12.0	−15.2	−5.24	1.05
Jarosite-Na	−12.4	−17.3	−13.9	−17.2	−7.06	0.55
Gypsum	−0.20	−0.07	−0.76	−0.46	−0.38	0.43
Melanterite	−3.39	−4.94	−5.63	−5.41	−6.11	−3.97
Lead minerals						
Anglesite	−2.92	−2.88	−3.79	−4.60	−1.03	−0.49
Cotunnite	−4.98	−4.75	−6.10	−6.31	−2.57	−2.93
Cerrusite	−1.35	−1.86	−2.97	−1.94	0.76	−2.90
Zinc minerals						
Goslarite	−6.93	−6.56	−7.36	−7.58	−6.25	−5.32
Other minerals						
Chalcanthite	−15.0	−15.1	−12.4	−17.3	−11.5	−7.1
Fayalite	−11.6[a]	−12.8[a]	−13.3[a]	−8.36[a]	−8.96[a]	−35.4

Saturation indices calculated using PHREEQC and database MINTEQ.
[a] Forsterite.

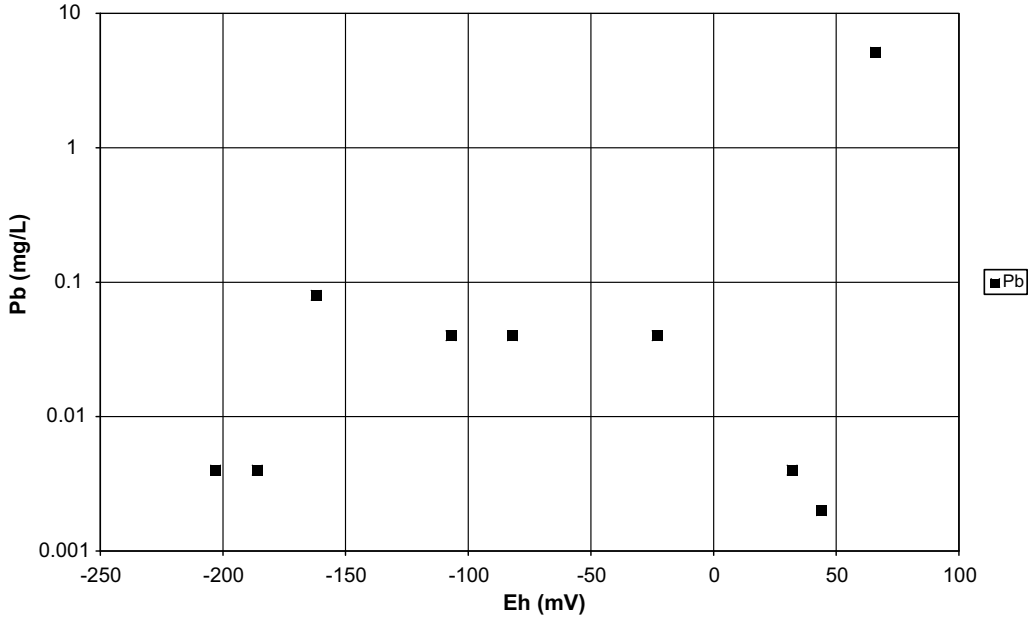

Fig. 10. Relationship between Eh and dissolved Pb in contaminated groundwater.

reducing conditions and low pH prevail, $H_3AsO_3^0$ may be the dominant species and dissolved As may be present in the As(III) form (Table 5).

The high Fe, Pb and Zn contents in the contaminated waters might, therefore, be related to the dissolution of secondary phases present in the slags (Table 6), as occurs in the tailings and contaminated soils surrounding the main mining area of Sierra Almagrera (Navarro et al., 2004). The flux of contaminants reaching the beach and shallow marine sediments was estimated based on the hydraulic gradient, the hydraulic conductivity of the porous media and the saturated surface of the studied aquifer. Using a Darcy velocity of 0.78 m/day, the theoretical stationary flow of contaminants is estimated at 1900 kg/ for Fe, 5 kg/a for Pb and 340 kg/a for

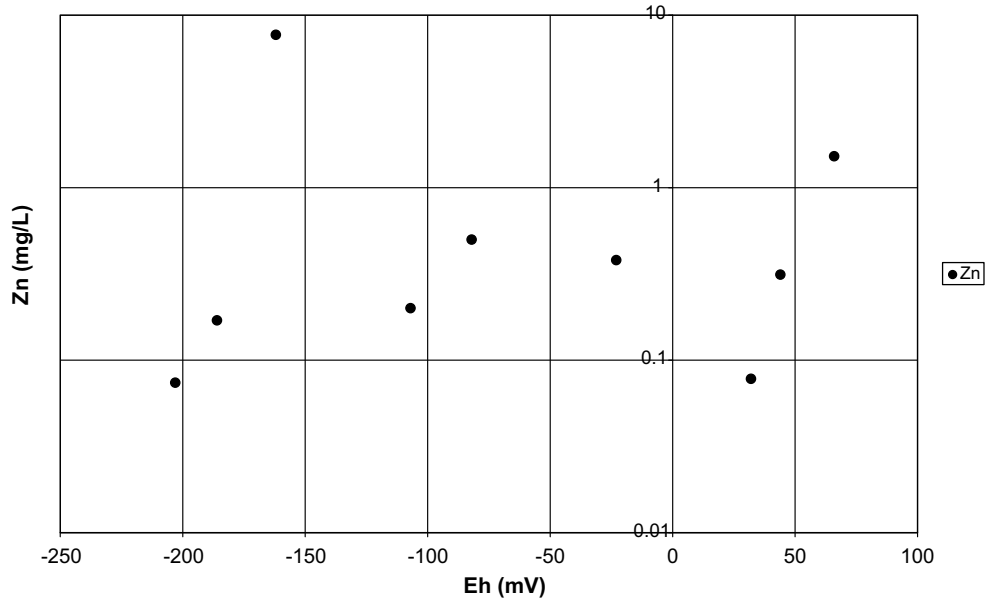

Fig. 11. Relationship between Eh and dissolved Zn in contaminated groundwater.

Zn. This result is consistent with that of Guerrero et al. (1990) who found significant amounts of metals (Hg: 0.55 ppm, Mn > 200 ppm, Pb: 80 ppm) in the superficial marine sediments near the Sierra Almagrera Coast.

4.4. Leaching test and geochemical modeling

The results of leaching tests (Table 7) show significant solubilization of metals, metalloids and other inorganic compounds (Na, Mg, K and Sr). Thus, Al (0.89–12.6 mg/L), Mn (0.85–40.2 mg/L), Fe (0.22–9.8 mg/L), Zn (>2.5 mg/L) and Pb (>2 mg/L) are mobilized in quantities similar to those found in the most contaminated aquifer wells (Table 7).

Elements such as As (5.2–31 μg/L), Cu (>2 mg/L), Ni (0.092–2.7 mg/L) and Sb (3.4–11.6 μg/L) were also leached from the slags used in the tests, although in higher amounts than those found in the groundwater, which might be related to an attenuation process in the aquifer. Finally, in the leaching tests, Ag (0.2–31 μg/L), Cd (1.3–36.8 μg/L) and Hg (0.2–7 μg/L) were detected, although these metals were not found in the analyzed groundwaters. The concentrations of dissolved metals are higher than the values reported in slag dumps of Penn mine and in leachates of the Clayton Ag mine (Table 7), with the exception of Pb and Zn, perhaps reflecting a more intense weathering of the slags in the study area.

Secondary minerals seem to play a very important role in the mobility of metals and trace elements.

Table 7
Main hydrogeochemical characteristics of leachates obtained in the column-leaching experiment and two water samples from US slag dumps

Parameter	Penn mine (1)	Clayton silver mine (2)	Leaching experiment
pH	7.2	5.65	5.39–6.4
Mg (mg/L)	1.4	<0.1	5.52–1290
Na	2.10	0.25	21.9–11,900
K	0.92	0.34	3.18–19.8
SO_4	7.4	4.7	200–17,500
Al (μg/L)	21	7.1	893–12,600
As	0.72	52	5.2–31
Ba	140	5	55–101
Cd	0.41	0.3	1.3–36.8
Cu	4.6	650	200 → 2000
Fe	41	<20	220–9800
Mn	7.6	120	854–40,200
Ni	0.55	3	92.2–2760
Pb	0.53	8400	200–2000
Sb	2.1	230	3.4–11.6
Zn	250	310	200 → 2500

(1) Water chemistry from depression in a slag dump (Parsons et al., 2001).
(2) Leachate sample from Pb–Ag Clayton silver mine obtained by deionized water (Piatak et al., 2004).

Major cation units are mg/L and minor elements units are μg/L.

Particular salts are formed at every dumping area depending on the local composition, pH and Eh of groundwater and the relative humidity. The heavy metal mobilization and/or attenuation processes resulting from the interaction between groundwater

and smelter slags vary according to the composition of the slag (Ettler et al., 2003).

The chemical analysis of leachate D1 was used to evaluate the speciation of dissolved constituents and to calculate the saturation state of the effluents (Tables 5 and 6). The numerical code PHREEQC (version 2.10.03) was used for these calculations.

In relation to Fe phase minerals, the modeling of leachate D1 indicates that ferrihydrite and goethite are undersaturated, and $Fe(OH)_{2.7}Cl_{0.7}$, jarosite and natrojarosite are supersaturated, unlike in groundwater, where hydroxysulfates are clearly undersaturated. Melanterite, which has a behaviour similar to other efflorescent salts detected in the mineralogical study (halotrichite, szomolnokite, etc.) is also undersaturated, indicating a control of Fe-solubility by Fe hydroxysulfates and the possible dissolution of oxyhydroxides and efflorescent salts during the leaching process. The primary phase fayalite is undersaturated as well, and a kinetic rate of surface-controlled dissolution of the silicate can explain part of the dissolved Fe, such as in other base-metal slag dumps (Parsons et al., 2001).

The mobilization of As, Cu, Ni and Zn in the leachates may be related to the dissolution of undersaturated secondary phases and primary mineral phases such as melilite and/or celsian for Zn, because of the great concentration of ZnO in these minerals (up to 2.5 wt.%). As for secondary phases, Cu and Zn may originate in the dissolution of chalcanthite and goslarite, while As and Ni can be mobilized from efflorescent salts in the weathered slags (copiapite, halotrichite and szomolnokite).

The dissolved concentrations of some anions such as SO_4^{2-} and some cations (Na^+, Mg^{2+}) detected in the leachates might reflect the hydrogeochemistry of the "pore water". Thus, the soil and slag "pore water" may be affected by seawater infiltration from the present industrial activity, thereby causing the mobilization of these substances in the leaching experiment.

5. Conclusions

This study examined the role of unconfined slag dumps from the old mining district of Sierra Almagrera (Almería, SE Spain) in the contamination of soils and groundwaters. Geochemical and mineralogical analyses show that smelting slags and soils in the vicinity of SA contain high concentrations of Ag, As, Ba, Cu, Fe, Pb, Sb and Zn.

The slag textures consist of a matrix of prismatic silicate crystals (olivine, celsian and melilite) and rounded sulfide blebs (pyrrhotite, sphalerite and galena) distributed throughout the samples. Cotunnite, magnetite, goethite and Zn–Pb–Fe alloys appear scattered throughout the matrix and along silicate grain boundaries.

Quartz, fayalite, barite, melilite, celsian, pyrrhotite, magnetite, galena and Zn–Pb–Fe alloys occur as primary phases and jarosite–natrojarosite, cotunnite, cerussite, goethite, ferrihydrite, chalcanthite, copiapite, goslarite, halotrichite and szomolnokite occur as secondary phases. Olivines are Fe-rich (Fa_{82}), containing up to 1.5 wt.% ZnO. Celsian contains up to 30.5 wt.% BaO and reflects the presence of abundant barite in the ores. Amounts of Pb (up to 0.4 wt.% PbO) and Zn (up to 2.5 wt.% ZnO) were also found in this mineral. Melilite is Ba–Fe-rich (up to 21 and 22 wt.% BaO and FeO_T, respectively) and contains up to 2.5 wt.% ZnO. The origin of cotunnite is not well understood, but it probably formed after the reaction of Pb-bearing minerals (galena) with the seawater used by chemical industrial facilities located on top of the slag dumps. Sea water probably accelerated metal mobilization in this study area by causing an ionic strength increase in the pore water. The formation of Cl species and minerals such as cotunnite, may promote the mobilization of metals that would otherwise have low mobility.

Due to their reactivity, sulfide blebs may be a major source of metal contamination. However, in semiarid environments such as the study area, the role of secondary phases (Fe–Cu sulfates such as chalcanthite, copiapite, halotrichite and szomolnokite) accumulated in soils and mining residues during dry periods seems very important in the mobilization of Cu, Pb and Zn, as demonstrated in laboratory experiments (Navarro et al., 2004). Groundwater below the main dumping area contains high amounts of Cu (0.64 mg/L), Fe (40 mg/L), Mn (0.6 mg/L), Pb (5.1 mg/L), Zn (7.6 mg/L) and As (0.019 mg/L). The oxidation of sulfides from the slag dumps contributed to the development of acidic waters that mobilized these metals into the groundwater, soil and marine environment.

Leaching experiments using demineralized water provided an experimental analog for the solubilization of metals from slags, thus confirming the mobilization of heavy metals from slag minerals. The release of metals and trace elements into the aquifers, soils and seawater along the coastline seems

to be controlled by the dissolution of metal sulfates and oxyhydroxides originating from the oxidation of sulfides. If the leaching tests reproduce the mobilization of metals that can be released from the slag in environmental conditions, the impact over the sediments and marine environment may be very important.

Acknowledgements

This study was supported by an economic agreement between the Technical University of Catalonia (UPC) and the private sector (Project C-5503) and by the Spanish Ministry of Science and Technology (Projects REN2003–09247-C04-03 and ENE2006-13267-C05-03) in collaboration with the Research Center for Energy, Environment and Technology (CIEMAT). The leaching experiments carried out by the staff of the Department of Fluid Mechanics (UPC) are gratefully acknowledged. The authors would like to thank two anonymous reviewers for the thorough review of the manuscript and, especially, to Richard Wanty for their useful suggestions.

References

APHA, 1989. Standard Methods for the Examination of Water and Wastewater, 17th ed. APHA, Washington.

Balistrieri, L.S., Box, S.E., Bookstrom, A.A., 2002. A geoenvironmental model for polymetallic vein deposits: a case study in the Coeur d'Alene mining district and comparisons with drainage from mineralized deposits in the Colorado Mineral Belt and Humboldt Basin, Nevada. US Geol. Surv. Open File, Report 02-195, pp. 143–160.

Bell, D.F., Donnelly, L.J., 2006. Mining and its Impact on the Environment. Taylor & Francis, Abingdon, Oxon, UK.

Bhandari, A., Surampalli, R.Y., Champagne, P., Ong, S.K., Tyagi, R.D., Lo, I.M.C., 2007. Remediation Technologies for Soils and Groundwater. ASCE, Reston, Virginia.

Bigham, J.M., Nordstrom, D.K., 2000. Iron and aluminum hydroxysulfates from acid sulfate waters. In: Alpers, C.N., Jambor, J.L., Nordstrom, D.K. (Eds.), Sulfate Minerals: Crystallography, Geochemistry, and Environment Significance, Reviews in Mineralogy and Geochemistry, vol. 40. Mineralogical Society of America, Geochemical Society, Washington, pp. 351–403.

Blowes, D.W., Ptacek, C.J., Benner, S.G., McRae, C.W.T., Bennet, T.A., Puls, R.W., 2000. Treatment of inorganic contaminants using permeable reactive barriers. J. Contam. Hydrol. 45, 123–137.

Deer, W.A., Howie, R.A., Zussman, J., 1975. An Introduction to the Rock-Forming Minerals. Longman, London.

Ettler, V., Piantone, P., Touray, J.C., 2003. Mineralogical control on inorganic contaminant mobility in leachate from lead–zinc metallurgical slag: experimental approach and long-term assessment. Mineral. Mag. 67, 1269–1283.

Guerrero, J., Rodríguez, C., Deyá, M., Jornet, A. 1990. Metales pesados en sedimentos marinos del golfo de Vera (Almería). Informes Técnicos del Instituto Español de Oceanografía 83, Ministerio de Agricultura Pesca y Alimentación, Madrid.

Jambor, J.L., Nordstrom, D.K., Alpers, C.N., 2000. Metal-sulfate salts from sulfide mineral oxidation. In: Alpers, C.N., Jambor, J.L., Nordstrom, D.K. (Eds.), Sulfate Minerals: Crystallography, Geochemistry, and Environment Significance, Reviews in Mineralogy and Geochemistry, vol. 40. Mineralogical Society of America, Geochemical Society, Washington, pp. 303–350.

Jurjovec, J., Ptacek, C.J., Blowes, D.W., 2002. Acid neutralization mechanisms and metal release in mine tailings: a laboratory column experiment. Geochim. Cosmochim. Acta 66, 1511–1523.

Kucha, H., Martens, A., Ottenburgs, R., De Vos, W., Viaene, W., 1996. Primary minerals of Zn–Pb mining and metallurgical dumps and their environmental behavior at Plombières, Belgium. Environ. Geol. 27, 1–15.

Lindsay, W., 1979. Chemical Equilibria in Soils. John Wiley and Sons, New York.

Martínez, J., García, J., López Ruiz, J., Reynolds, G.A., 1992. Discovery of fossil fumaroles in Spain. Econ. Geol. 87, 444–447.

Maskall, J., Whitehead, K., Gee, C., Thornton, I., 1996. Long-term migration of metals at historical smelting sites. Appl. Geochem. 11, 43–51.

Ministry of Housing Spatial Planning and Environment, 2000. Circular on target values and intervention values for soil remediation. DBO/1999226863, The Hague.

Morales, S., 1994. Estudio de los yacimientos de metales base de las zonas de Águilas y Sierra Almagrera. Doctoral thesis, Univ. Granada. Unpubl.

Navarro, A., Biester, H., Mendoza, J.L., Cardellach, E., 2006b. Mercury speciation and mobilization in contaminated soils of the Valle del Azogue Hg mine (SE, Spain). Environ. Geol. 49, 1089–1101.

Navarro, A., Chimenos, J.M., Muntaner, D., Fernández, I., 2006a. Permeable reactive barriers for the removal of heavy metals: lab-scale experiments with low-grade magnesium oxide. Ground Water Monitor. Remed. 26, 142–152.

Navarro, A., Collado, D., Carbonell, M., Sánchez, J.A., 2004. Impact of mining activities in a semi-arid environment: Sierra Almagrera district, SE Spain. Environ. Geochem. Health 26, 383–393.

Navarro, A., Collado, D., Sánchez, J.A., 1998. Análisis de la contaminación por actividades mineras de los suelos de la cuenca baja y delta del río Almanzora. Boletín Geológico y Minero 109, 69–87.

Navarro, A., Martínez, J., Font, X., Viladevall, M., 2000. Modelling of modern mercury vapor transport in an ancient hydrothermal system: environmental and geochemical implications. Appl. Geochem. 15, 281–294.

Navarro, A., Viladevall, M., Font, X., Rodríguez, P., 1994. Las mineralizaciones auríferas de Sierra Almagrera (Almería). Estudio geoquímico y modelos de yacimientos. Boletín Geológico y Minero, 85–101.

Parkhurst, D.L., Appelo, C.A.J., 1999. User's Guide to PHREEQC (version 2): A Computer Program for Speciation, Batch-Reaction, One-Dimensional Transport, and Inverse Geochemical Calculations. US Geol. Surv., Water-Resour. Investig. Report, 99-4259.

Parsons, M.B., Bird, D.K., Einaudi, M.T., Alpers, C.N., 2001. Geochemical and mineralogical controls on trace element release from the Penn Mine base-metal slag dump, California. Appl. Geochem. 16, 1567–1593.

Piatak, N.M., Seal II, R.R., Hammarstrom, J.M., 2004. Mineralogical and geochemical controls on the release of trace elements from slags produced by base- and precious-metal smelting at abandoned mine sites. Appl. Geochem. 19, 1039–1064.

Rieuwerts, J., Farago, M., 1996. Heavy metal pollution in the vicinity of a secondary lead smelter in the Czech Republic. Appl. Geochem. 11, 17–23.

Schmidt, R.G., Ager, C.M., Montes, J.G., 2001. More than broken jars and roof tiles, the environmental legacy of a Roman mineral industry at Plasenzuela, Extremadura, Spain. Project: Long-term environmental effects of Roman mining in the Plasenzuela silver–lead district of Extremadura, Spain. US Geol. Surv. website: <http://minerals.usgs.gov/east/plasenzuela/background.shtml>.

Seal, R.R., Hammarstrom, J.M., 2003. Geoenvironmental models of mineral deposits: examples from massive sulfide and gold deposits. In: Jambor, J.L., Blowes, D.W., Ritchie, A.I.M. (Eds.), Environmental Aspects of Mine Wastes, Mineralogical Association of Canada, vol. 31, pp. 11–50.

Smedley, P.L., Kinniburgh, D.G., 2002. A review of the source, behaviour and distribution of arsenic in natural waters. Appl. Geochem. 17, 517–568.

Viladevall, M., Font, X., Navarro, A., 1999. Geochemical mercury survey in the Azogue Valley (Betic area, SE Spain). J. Geochem. Explor. 66, 27–35.